Molecular Plant Advance Access published August 30, 2013

PtrCel9A6, an Endo-1,4-β-Glucanase, Is Required for Cell Wall Formation during Xylem Differentiation in *Populus*

Liangliang Yu, Jiayan Sun and **Laigeng Li**[1]

National Key Laboratory of Plant Molecular Genetics/CAS Key Laboratory of Synthetic Biology, Institute of Plant Physiology and Ecology, Shanghai Institutes for Biological Sciences, Chinese Academy of Sciences, 300 Fenglin Road, Shanghai 200032, China

ABSTRACT Endo-1,4-β-glucanases (EGases) are involved in many aspects of plant growth. Our previous study found that an EGase, PtrCel9A6, is specifically expressed in differentiating xylem cells during *Populus* secondary growth. In this study, the xylem-specific PtrCel9A6 was characterized for its role in xylem differentiation. The EGase is localized on the plasma membrane with catalytic domain toward the outside cell wall, hydrolyzing amorphous cellulose. Suppression of *PtrCel9A6* expression caused secondary cell wall defects in xylem cells and significant cellulose reduction in *Populus*. Heterologous expression of *PtrCel9A6* in *Arabidopsis* enhanced plant growth as well as increased fiber cell length. In addition, introduction of *PtrCel9A6* into *Arabidopsis* resulted in male sterility due to defects in anther dehiscence. Together, these results demonstrate that PtrCel9A6 plays a critical role in remodeling the 1,4-β-glucan chains in the wall matrix and is required for cell wall thickening during *Populus* xylem differentiation.

Key words: endo-1,4-β-glucanase; cell wall; cellulose synthesis; cell wall thickening; *Populus*.

INTRODUCTION

Endo-1,4-β-glucanase (EGase, EC 3.2.1.4), often referred to as cellulase, hydrolyzes 1,4-β-D-glucan chain molecules and plays a role in various physiological processes. EGase genes are found in many prokaryotic and eukaryotic organisms, including bacteria, fungi, slime molds, nematodes, animals, and plants (Levy et al., 2002; Libertini et al., 2004). In plants, EGases are encoded by a large gene family, belonging to the glycosyl hydrolase gene family 9 (GH9) (Henrissat, 1991). According to their sequence domain structure, this multigene family can be grouped into three subclasses: A subclass (GH9A), membrane-anchored GH9; B subclass (GH9B), secreted GH9; and C subclass (GH9C), secreted proteins with a carbohydrate binding module, CBM49 (Urbanowicz et al., 2007). Alternatively, the plant EGase gene family can be divided into α, β, and γ subfamilies based on phylogenetic analysis (Libertini et al., 2004). In *Arabidopsis*, the α-subfamily mainly consists of secreted GH9 proteins (including GH9B and GH9C subclasses) except for one GH9A subclass protein. All γ-subfamily members are transmembrane proteins, belonging to GH9A subclass. Due to a lack of experimental data and clear typical domain prediction, it is unclear whether the β-subfamily proteins are membrane-anchored or secreted.

The α-subfamily contains the vast majority of EGases identified to date. A number of studies have documented the role α-subfamily EGases play in cell wall disassembly during the process of fruit ripening and abscission as well as in wall reconstruction during cell expansion (del Campillo, 1999; Rose and Bennett, 1999). Cell wall polysaccharides undergo considerable depolymerization during fruit ripening (Odonoghue and Huber, 1992; Maclachlan and Brady, 1994; Brummell and Harpster, 2001). Cellulase activity has been identified in the fruits of a number of plant species and is believed to contribute the disassembly of the cell wall during fruit softening (Brummell and Harpster, 2001). For example, cellulase was shown to contribute directly to the fruit ripening process in avocado (Pesis et al., 1978). Incubating unripe avocado fruit with purified Cx-cellulase caused a downshift in the molecular weight of cell wall polymers, an increase in the proportion of crystalline cellulose, and a loss of cohesiveness between cellulose fibrils, which suggested cleavage activity at non-crystalline regions of the microfibril (Odonoghue et al., 1994). High cellulase activity is also found to be associated

[1]To whom correspondence should be addressed. E-mail lgli@sibs.ac.cn, tel. 86-21-54924151, fax 86-21-54924015.

doi:10.1093/mp/sst104

Received 28 March 2013; accepted 29 May 2013

with the abscission zone where organ abscission occurs (Horton and Osborne, 1967) and a pI 9.5 cellulase is reported to contribute to the breakdown of the cell wall during abscission (Sexton et al., 1980). Two divergent EGase genes, *LeCel1* and *LeCel2*, exhibit overlapping expression during fruit ripening and organs abscission in tomato (Lashbrook et al., 1994). Individual suppression of *LeCel1* and *LeCel2* expression in the abscission zone reduced floral and fruit abscission, respectively (Lashbrook et al., 1998; Brummell et al., 1999).

α-type EGases are also reported to play a role in accelerating cell growth through cell wall loosening (Cosgrove, 2005). Expression of the EGase gene *Cel4* was found to be highly correlated with rapid cell expansion in the pistils, hypocotyls, and leaves of tomato (Brummell et al., 1997a). In *Arabidopsis*, an α-type EGase gene (*Cel1*) was found to be expressed specifically in young expanding tissue (Shani et al., 2006) and down-regulation of *Cel1* expression resulted in shorter stems and roots (Tsabary et al., 2003). Heterologous overexpression of *Cel1* was able to enhance plant growth in poplar (Shani et al., 2004). Expression of *PopCel1* and *PopCel2* in poplar is associated with cell growth (Ohmiya et al., 2000, 2003).

The γ-subfamily EGases, which include KORRIGAN proteins (KOR), have a transmembrane domain near the N-terminus (Molhoj et al., 2002). The involvement of KOR in cellulose synthesis or accumulation has been reported in a number of plant species, including *Arabidopsis*, poplar, rice, and white spruce (Sato et al., 2001; Szyjanowicz et al., 2004; Zhou et al., 2006; Maloney and Mansfield, 2010; Maloney et al., 2012). *KOR1* mutants (*kor1-1*, *acw1*, *irx2*) in *Arabidopsis* exhibit defects in cellulose accumulation and abnormal formation of both primary and secondary walls (Nicol et al., 1998; Sato et al., 2001; Szyjanowicz et al., 2004). A stronger *KOR1* mutant allele (*kor1-2*) also exhibits defects during cytokinesis due to aberrant cell plate formation (Zuo et al., 2000). *KOR* affects cellulose crystallinity in cell walls (Takahashi et al., 2009; Maloney and Mansfield, 2010). The KOR protein exhibits specific cellulase activity on low substituted cellulose derivatives and amorphous cellulose, but not on crystalline cellulose or other polysaccharides *in vitro* (Molhoj et al., 2001; Master et al., 2004). Compared to the α/γ-subfamilies, EGases within the β-subfamily contain different sequence structures and have been little studied in plants.

In a previous study, we reported identification of a β-subfamily EGase gene, *PtrCel9A6*, in the plasma membrane proteins of secondary vascular tissues in *Populus* (Song et al., 2011). The present paper further examines the physiological function of this β-subfamily EGase gene in *Populus* secondary growth.

RESULTS

Identification and Expression of *PtrCel9A6* in *Populus trichocarpa*

In our previous study, we detected a β-subfamily EGase protein in the plasma membrane of differentiating *Populus* vascular tissues (Song et al., 2011). Cloning of the EGase gene indicated that it encoded a putative 57.2-kD protein with 523 amino acids. The gene was named *PtrCel9A6* according to the suggested nomenclature (Urbanowicz et al., 2007).

Plant endo-1,4-β-glucanase enzymes are encoded by the GH9 gene family. Twenty-seven putative GH9 genes (Supplemental Table 1), one more than the previously reported number (Takahashi et al., 2009), were identified in the *Populus* genome sequence (www.phytozome.net/poplar). As in *Arabidopsis* (Libertini et al., 2004), the GH9 genes in *Populus* can be classified into three subfamilies (α, β, γ) (Supplemental Figure 1A). The β-subfamily contains *PtrCel9A6*, *PtrGH9A7*, and *PtrGH9A8*, with *PtrCel9A6* and *PtrGH9A7* forming a duplicated pair, which share an 86% amino acid sequence identity (Supplemental Figure 1A and 1B). To examine the expression profile of *PtrCel9A6*, quantitative RT–PCR was carried out using nine *P. trichocarpa* tissues, including developing xylem, phloem, cork (mainly epidermis and cortex), young leaf, mature leaf, leaf vein, petiole, root, and shoot tip. Results showed that *PtrCel9A6* was highly and specifically expressed in differentiating xylem but expressed at a basal level in phloem, cork, shoot tip, and leaves. Moderate expression was detected in leaf vein, petiole, and root, which contain xylem tissue (Figure 1A). The expression

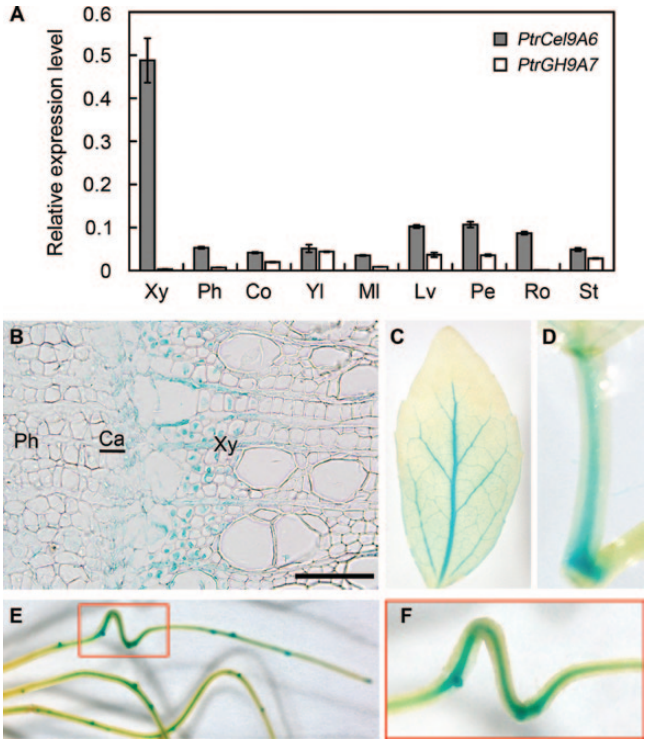

Figure 1. Expression Profile of *PtrCel9A6*.
(A) Quantitative RT–PCR expression analysis of *PtrCel9A6* and its duplicated gene *PtrGH9A7* in various *Populus* tissues. *Populus Actin2* was used as a reference for normalization.
(B–F) GUS staining in various organs of *PtrCel9A6pro:GUS* transgenic *Populus*, **(B)** in early differentiating xylem, **(C)** in vascular bundle of young leaf blade, **(D)** in petiole, and **(E,F)** in root steles and lateral root primordia. Xy, differentiating xylem; Ph, differentiating phloem; Co, cork; Yl, young leaf; Ml, mature leaf; Lv, leaf vein; Pe, petiole; Ro, root; St, shoot tip; Ca, cambium. Bar = 100 μm.

pattern of *PtrGH9A7* differed from that of *PtrCel9A6*, though the two genes are a duplicated pair (Figure 1A).

To verify the specificity of *PtrCel9A6* expression, a 2.4-kb promoter fragment from the *PtrCel9A6* gene was cloned and fused to the *GUS* gene. The fusion construct was then transformed into *Populus.* Analysis of the GUS staining showed that the *PtrCel9A6* promoter is specifically active in differentiating xylem but not in other tissues such as cortex, phloem (including phloem fiber cells), mature xylem, and pith in stem. Within the differentiating xylem, higher GUS activity was detected in the differentiating fiber and vessel cells which were undergoing secondary cell wall thickening compared to the early expanding xylem cells adjacent to the cambium zone (Figure 1B). GUS activity was also specifically detected in the vascular bundles of leaf and root (Figure 1C–1F). We also noticed that GUS activity in the root appeared in lateral root primordium as well as in stele (Figure 1E and 1F). Together, these results demonstrate that *PtrCel9A6* is expressed mainly in differentiating vascular tissues, likely in differentiating xylem cells specifically.

It is known that α and γ subfamily members display distinct functions *in planta*. Comparison of PtrCel9A6 with γ-subfamily members, PtrCel9A1/PtrKOR1 and AtGH9A1/KOR1 (Nicol et al., 1998; Takahashi et al., 2009), and α-subfamily members, PtrCel9B1/PopCel1 and AtGH9B1/Cel1 (Nakamura et al., 1995; Shani et al., 1997), revealed that they contain distinct N-terminal sequences while the GH9 catalytic domains are conserved (Supplemental Figure 1B). There is a signal peptide in PtrCel9B1 and AtGH9B1 but a putative transmembrane domain in PtrCel9A6 and PtrGH9A7, similar to PtrCel9A1 and AtGH9A1 (Supplemental Figure 1B). This suggests that the subcellular localization of PtrCel9A6 and PtrGH9A7 is similar to that of KORs but different from that of secreted α-type members. However, PtrCel9A6 and PtrGH9A7 do not contain an N-terminal cytosolic tail and polarized targeting signals which are conserved in KOR proteins (Supplemental Figure 1B) (Zuo et al., 2000; Maloney and Mansfield, 2010). The different domain structures of the β-type proteins suggest their function in plants differ from those of α and γ subfamily members.

Subcellular Localization of PtrCel9A6

Analysis of the PtrCel9A6 sequence by the TMHMM 2.0 and SignalP 4.0 programs indicated that PtrCel9A6 possesses a transmembrane domain near its N-terminus and a GH9 catalytic domain out of the plasma membrane, facing the cell wall, but no obviously detectable signal peptide sequence (Supplemental Figure 2A and 2B). This prediction is consistent with its isolation from the plasma membrane (Song et al., 2011). To further verify its subcellular localization, a construct coding for a PtrCel9A6–GFP fusion protein was generated under the control of a cauliflower mosaic virus (CaMV) 35S promoter. The construct was introduced into tobacco leaf through *Agrobacterium*-mediated transformation. Protein location assay demonstrated that PtrCel9A6 is localized on the plasma membrane (Figure 2B and 2C). The *35S: PtrCel9A6* construct was transferred into *Arabidopsis*. Western blot analysis showed that the PtrCel9A6 protein was detected in the microsomal fraction of the leaf protein isolated from transgenic *Arabidopsis*. Treatment of the microsomes with sodium carbonate at pH 11.5, a procedure known to convert the microsomal vesicles to open membrane sheets and release peripheral membrane proteins (Fujiki et al., 1982), showed that PtrCel9A6 was retained in the membrane fraction (Figure 2D). Therefore, these results demonstrate that PtrCel9A6 is an integral plasma membrane protein.

PtrCel9A6 Enzymatic Activity

As the *PtrCel9A6* gene was predicted to code an EGase, its ability to hydrolyze polysaccharides containing 1,4-β-D-glucan linkages was investigated. When the PtrCel9A6 recombinant protein was generated in the *Escherichia coli* system, we could not detect its enzyme activity. We then transformed *Arabidopsis* with the *35S: PtrCel9A6* construct. Extract from the young leaves of the transgenic plants contained large amounts of PtrCel9A6 protein (Figure 3B) and were used to determine the hydrolysis activity of PtrCel9A6. Carboxymethyl cellulose (CMC) was used as a substrate for EGase activity determination. Significant hydrolysis activity was detected with the protein from the transgenic leaves, but a trivial level of activity was observed in wild-type (WT) leaves (Figure 3A). This suggests the PtrCel9A6 protein produced in *Arabidopsis* leaves is active in cleaving the 1,4-β-glucan linkage. The substrate specificity of PtrCel9A6 was determined using various cellulose derivatives and other cell wall polysaccharides. As shown in Figure 3C, PtrCel9A6 had the highest activity with CMC substrate, moderate activity with phosphoric acid swollen cellulose, and low

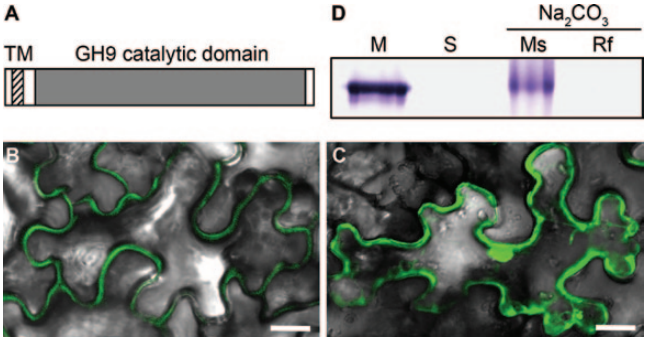

Figure 2. Analysis of PtrCel9A6 Plasma Membrane Localization.
(A) Schematic structure of the predicted domains in PtrCel9A6. TM, transmembrane domain.
(B) Expression of *35S:PtrCel9A6-GFP* fusion protein in tobacco leaf epidermal cells.
(C) Expression of *35S:GFP* protein as control.
(D) Western blotting proteins from transgenic *Arabidopsis* leaves expressing *PtrCel9A6*, showing PtrCel9A6 is present in microsomal (M), not in soluble fraction (S). After microsomal was treated with sodium carbonate, showing that PtrCel9A6 is retained in membrane sheet (Ms), not in the removed fraction by the treatment (Rf). Bars = 20 μm.

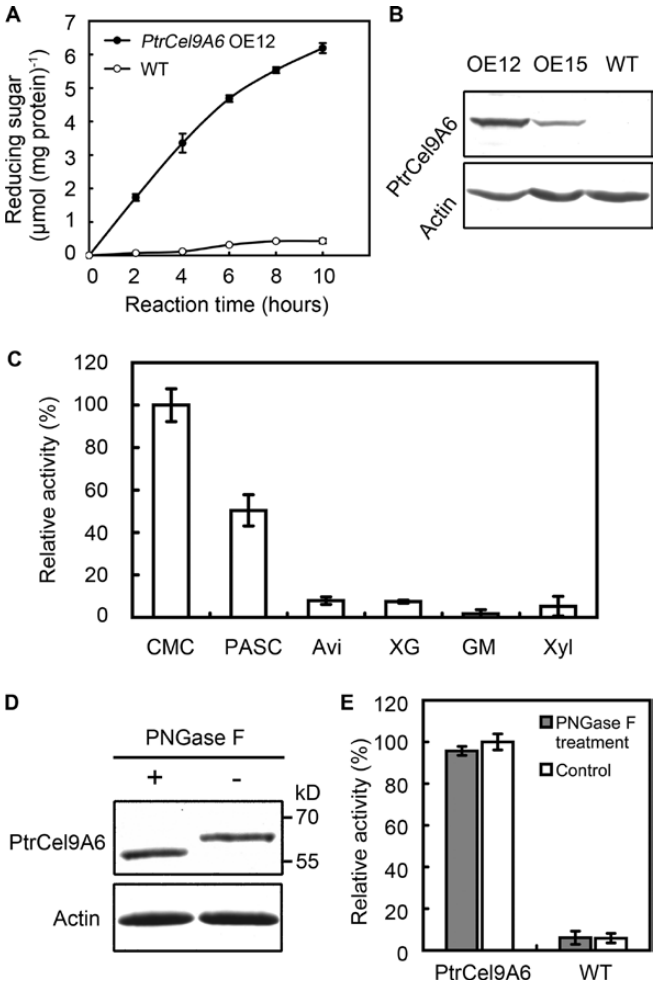

Figure 3. Enzyme Properties of PtrCel9A6.
(A) Hydrolyzing activity of PtrCel9A6 isolated from the leaves of *PtrCel9A6*-overexpressed *Arabidopsis*; WT, proteins from wild-type *Arabidopsis*. The values are means ± SE of three biological replicates of each line.
(B) Western blotting of PtrCel9A6 in transgenic *Arabidopsis*, and antibodies against actin as a loading control.
(C) PtrCel9A6 activity on various substrates. CMC, carboxymethyl cellulose; PASC, phosphoric acid swollen cellulose; Avi, avicel; XG, xyloglucan; GM, glucomannan; Xyl, xylan.
(D) Western blotting of PtrCel9A6 with (+) and without (–) PNGase F treatment.
(E) Effect of PNGase F treatment on PtrCel9A6 activity. The values in (C) and (E) are means ± SE of triplicate sample measurements.

activity with microcrystalline cellulose avicel and xyloglucan. No activity with glucomannan or xylan was detected. The different hydrolytic activities with various polysaccharides shows PtrCel9A6 is active in hydrolyzing non-crystalline cellulose but minimally or not active in cleaving crystalline cellulose or other polysaccharides.

Four *N*-glycosylation sites were predicted in the PtrCel9A6 sequence (Supplemental Figures 1B and 2C). To examine PtrCel9A6 *N*-glycosylation, proteins extracted from the leaves of transgenic *Arabidopsis* were treated with PNGase F to remove *N*-liked glycan side-chains. After treatment, the PtrCel9A6 band size became smaller compared to the untreated protein (Figure 3D). The size of the treated protein is consistent with the predicted PtrCel9A6 molecular size which suggests PtrCel9A6 is modified by *N*-glycosylation. To examine the effect of glycosylation on PtrCel9A6 activity, enzymes extracted from transgenic *Arabidopsis* leaves were treated with PNGase F. Enzyme activity with CMC substrate did not show significant change compared to the untreated enzyme (Figure 3E). These results demonstrate that the *N*-linked oligosaccharide chains may not be necessary for PtrCel9A6 catalytic activity.

Effects of PtrCel9A6 on *Populus* Xylem Development

To analyze *PtrCel9A6* genetic function, expression of *PtrCel9A6* was specifically knocked down through RNAi suppression. *Populus* 'Nanlin 895' was used for genetic transformation and its *Cel9A6* gene coding sequence shares 98.5% identity with *PtrCel9A6* (Supplemental Figure 3). A specific fragment of 248 bp from the ATG code region (Supplemental Figures 1B and 3) was constructed to form a hairpin structure under the control of the CaMV 35S promoter. The construct was transferred into *Populus* and 30 independent transgenic lines were generated. Expression of *PtrCel9A6* was significantly down-regulated in six of the transgenic lines. Lines 6 and 17, which had the lowest *PtrCel9A6* transcript levels (Figure 4A), were used for detailed analysis. Given the high sequence similarity between *PtrCel9A6* and *PtrGH9A7*, the expression level of *PtrGH9A7* was examined as well. Results showed *PtrGH9A7* was significantly down-regulated in differentiating xylem (Supplemental Figure 4A). When plant height was measured every week in a greenhouse, slightly slower growth was observed in transgenic plants but without statistical significance compared to WT plants (Supplemental Figure 4C). Down-regulation of *PtrCel9A6* in transgenic lines did not cause obvious phenotypic alterations (Figure 4B). No significant differences in stem height and diameter, leaf length and width, and other traits were observed between transgenic and WT plants (Figure 4B and Supplemental Figure 4C and 4D). Considering the xylem-specific expression of the *PtrCel9A6* gene, stem cross-sections were examined. An 'irregular xylem' phenotype was observed in differentiating xylem tissues in the transgenic plants (Figure 4C–4E). This phenotype usually indicates a defect in secondary cell wall (SCW) biosynthesis. Transmission electron microscopy was applied to further examine the cell wall structure. The SCW was much thinner in the irregular vessel and fiber cells of the RNAi transgenic plants compared to WT plants (Figure 4F–4I). The SCW thickness of the fiber and vessel cells in the RNAi plants decreased by 52% and 45%, respectively (Figure 4J). Tensile strength was also reduced in the wood of the transgenic plants (Figure 4K). In addition, both holocellulose and α-cellulose content were reduced in *PtrCel9A6* down-regulated wood. The level of α-cellulose in particular was significantly reduced by 8–10% (Table 1). To differentiate the

effect of *PtrCel9A6* from the interference of *PtrCel9A1* which is reported to affect cell wall cellulose synthesis (Takahashi et al., 2009; Maloney and Mansfield, 2010), *PtrCel9A1* expression in developing xylem was examined and found to be not affected in the transgenics (Supplemental Figure 4B). These results suggest that *PtrCel9A6* plays a critical role in cellulose synthesis during xylem cell wall thickening.

PtrCel9A6 Overexpression in *Arabidopsis*

Transgenic *Arabidopsis* that constitutively overexpressed *PtrCel9A6* under the control of the 35S promoter were generated. Twenty independent transgenic lines were selected for analysis. Transcript levels measured by quantitative RT–PCR showed that *PtrCel9A6* was expressed in transgenic *Arabidopsis*. Among them, line 12 had the highest *PtrCel9A6* expression while line 15 showed moderate expression (Figure 5A). Their expression was further confirmed by Western blot analysis using antibodies against PtrCel9A6 (Figure 3B).

The sizes of the rosette leaves of the transgenic plants were bigger compared to control plants (Figure 5B and 5C, and Supplemental Figure 5C). Examination of the rosette

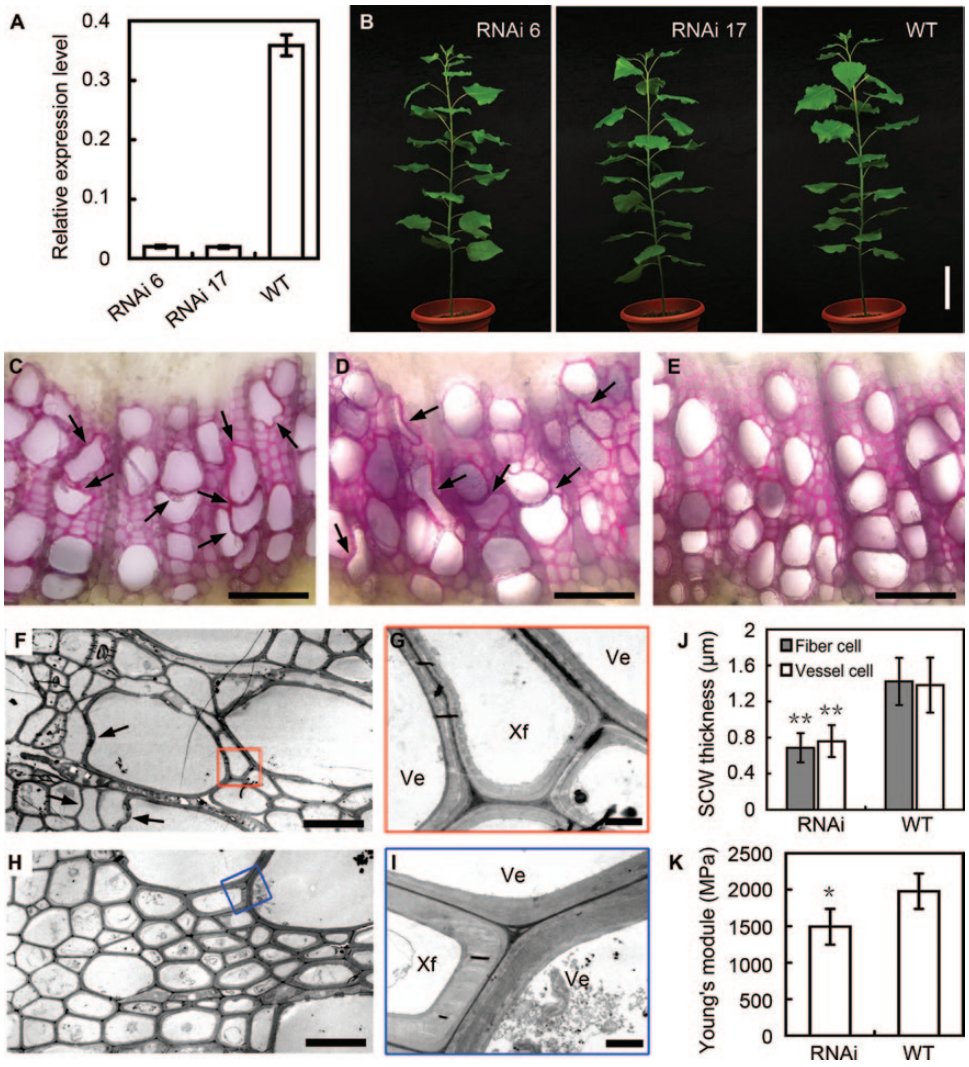

Figure 4. Effects of *PtrCel9A6* Down-Regulation on *Populus* Xylem Development.
(A) *PtrCel9A6* transcript level in the differentiating xylem of two *PtrCel9A6*-suppressed transgenic lines (RNAi 6 and RNAi 17).
(B) Morphology of RNAi 6 (left), RNAi 17 (middle), and wild-type (WT, right) in 10-week-old plants grown in a greenhouse.
(C–E) *Populus* stem (12th internode) cross-sections showed 'irregular xylem' phenotype (collapsed vessel elements, indicated by arrows) in RNAi 6 (C), RNAi 17 (D), and normal xylem development in WT (E).
(F–I) Transmission electron micrographs of the differentiating xylem cells of the RNAi (F) and WT (H) plants. (G, I) Enlargements of the boxed areas in (F) and (H), respectively. Arrow indicates irregular fiber and vessel cells. Xf, xylem fiber cell; Ve, vessel cell.
(J) SCW thickness of fiber and vessel cells. The values are means ± SE of 50 independent cells.
(K) Measurement of the tensile strength of wood. The values are means ± SE of 10 independent plants. Significance as determined by Student's *t*-test. * $P < 0.05$; ** $P < 0.01$. Bars = 10 cm in (B), 100 μm in (C–E), 20 μm in (F, H), 2 μm in (G, I).

leaf epidermal cells by scanning electron microscopy showed a significant enlargement of the cell size in the transgenic plants (Figure 5D and 5E). Enhanced cell expansion rather than cell proliferation appears to be the cause of the larger leaf size in the transgenic plants. In addition, the roots of the transgenic seedlings were approximately 1.5-fold longer as compared to WT (Supplemental Figure 5A and 5B). The transgenic plants grew larger (Figure 5F and 5G) after bolting (6-week-old). The dry weight of the biomass of the transgenic plant increased by 54% and 39% in transgenic lines 12 and 15, respectively (Figure 5H). The diameter of the basal part of the main inflorescence stem was enlarged in transgenic plants (Supplemental Figure 5D and 5E). The cells, especially the fiber and vessel cells in the stem cross-sections, were enlarged (Figure 5I and 5J) and the length of the fibers elongated in the transgenic stems (Figure 5K and Supplemental Figure 5F and 5G). These results demonstrate that overexpression of *PtrCel9A6* in *Arabidopsis* enhanced cell expansion and elongation and therefore resulted in an increase in plant growth and higher biomass production.

Abnormal Anther Dehiscence in the *PtrCel9A6* Overexpressed *Arabidopsis*

Shorter, empty siliques, and reduced fertility were observed in *PtrCel9A6* overexpressed *Arabidopsis* compared to WT (Figure 5F and 5G, and Figure 6A and 6B). The fertility rate of the transgenic plants was negatively correlated with *PtrCel9A6* expression levels. Line 15, which moderately expressed *PtrCel9A6*, had an 18% fertility rate while line 12, which highly expressed *PtrCel9A6*, had a 4% fertility rate (Figure 6C). Further examination of the flowering and reproductive organ structures revealed remarkable difference in anther dehiscence between the transgenic and WT plants. In WT plants, the release of pollen grains for pollination and fertilization occurred as usual after normal anther dehiscence (Figure 6E). In contrast, the anthers of the transgenics failed to dehisce despite the rupture of the stomium, causing the pollen grains to remain locked in its pollen sacs (Figure 6D). Pollen grains released from the unopened anthers were able to germinate and grow normally *in vitro* (Supplemental Figure 6A and 6B).

Anther development in *Arabidopsis* can be divided into 14 stages (Sanders et al., 1999). Transverse sections of transgenic anthers were examined at the different stages of development. Before stage 11, no noticeable morphological alterations were observed between transgenic and WT anthers (Figure 6F and 6G). Beginning from stage 11, when the endothecium of the WT started to deposit fibrous bands (wall thickenings), the endothecial layer in the transgenic anther failed to deposit fibrous bands (Figure 6H and 6I). At stage 13, the endothecium of the WT anthers had completed thickening, creating an outward bending force that causes the opening of the stomium to allow for pollen release (Figure 6K). However, the transgenic endothecium degenerated completely, resulting in a bilocular anther structure filled with pollen grains surrounded by a thin epidermal layer (Figure 6J). Expression of *AtGH9B5* and *AtGH9B7* (*Arabidopsis* orthologs of *PtrCel9A6*) at anther stage 11 to 12 was not affected in the transgenics (Supplemental Figure 6C). The failure to release pollen is therefore caused by the overexpression of *PtrCel9A6* which suppressed the thickening of the endothecium in *Arabidopsis*.

Table 1. Holocellulose and α-Cellulose Contents in *Populus* Xylem.

Line	Holocellulose (%)	α-cellulose (%)
RNAi 6	77.54 ± 0.40*	35.14 ± 0.49**
RNAi 17	74.75 ± 0.81**	34.30 ± 0.41**
WT	80.08 ± 1.16	38.24 ± 0.70

The values represent percentages based on the dry weight of the cell wall material. The values are means ± SE, $n = 5$ biological replicates for each line. Significance was determined by Student's *t*-test, * $P < 0.01$ and ** $P < 0.001$.

PtrCel9A6 Overexpression in *Populus*

The *PtrCel9A6* overexpression construct was also transformed into *Populus*. High expression of *PtrCel9A6* at both the transcript and protein levels was verified by quantitative RT–PCR and Western blot analysis (Figure 7A and 7B). No obvious morphological alterations in tree height, stem diameter, leaf area, xylem differentiation, and other traits were perceived between the transgenic and WT plants (Figure 7C). However, protein extracted from the transgenic leaves showed very weak hydrolysis activity (Figure 7D and Supplemental Figure 7C) in contrast to the high levels of PtrCel9A6 activity observed in transgenic *Arabidopsis* (Figure 3A and Supplemental Figure 7B). The phenomenon that production of more PtrCel9A6 protein in transgenic *Populus* (Supplemental Figure 7A) did not yield higher PtrCel9A6 activity remains to be further investigated.

DISCUSSION

PtrCel9A6 Is a Plasma Membrane-Anchored EGase which Hydrolyzes Amorphous Cellulose

EGases have been studied extensively in a number of plant species for their roles in the degradation and reconstruction of cell walls and cellulose accumulation (del Campillo, 1999; Rose and Bennett, 1999; Molhoj et al., 2002). However, all of the previously investigated EGases belong to either the α or γ subfamilies and the role of β-type EGases in plant remained largely unknown. Here, we studied the function of a poplar β-type EGase, PtrCel9A6. PtrCel9A6 is an integral membrane protein with its catalytic domain on the non-cytosolic side of the plasma membrane. The plasma membrane localization of PtrCel9A6 is different from that of α-type EGases, which are thought to be secreted to the cell wall, and γ-type EGases, which are located on the plasma membrane and/or

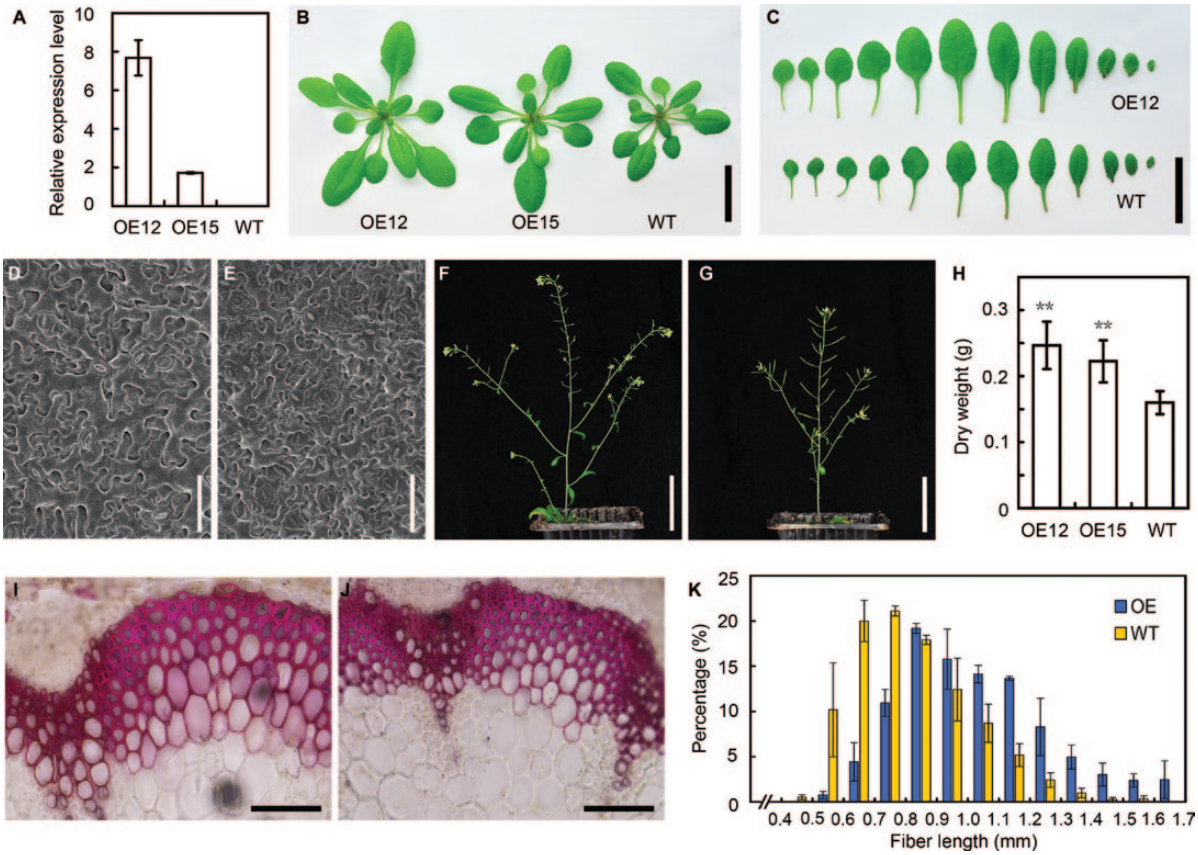

Figure 5. Effect of the *PtrCel9A6* Heterologous Expression in *Arabidopsis.*
(A) *PtrCel9A6* transcripts were measured by quantitative RT–PCR in *PtrCel9A6*-overexpressed (OE12, OE15) and wild-type (WT) *Arabidopsis*. The values are means ± SE of three plants of each line.
(B) OE12 (left), OE15 (middle), and WT (right) *Arabidopsis* at 4 weeks old.
(C) Rosette leaves in (B) (OE12 versus WT) from the first to last are arranged from left to right.
(D, E) Scanning electron micrographs of the leaf epidermal cells in OE12 (D) and WT (E).
OE12 **(F)** and WT **(G)** *Arabidopsis* at 6 weeks old.
(H) The dry weight of OE and WT *Arabidopsis* at 6 weeks old. The values are means ± SE, $n = 30$ replicates for each line.
Cross-sections stained with phloroglucinol-HCl in OE12 **(I)** and WT **(J)**.
(K) Length of fibers from the basal part of main inflorescence stems. More than 1000 fibers from three plants were measured for each line. Bar = 2 cm in (B, C), 50 μm in (D, E), 5 cm in (F, G), 100 μm in (I, J). Significance as determined by Student's *t*-test, ** $P < 0.01$.

intracellular compartment membranes (Brummell et al., 1997b; Nicol et al., 1998; Robert et al., 2005; Zhang et al., 2012). Differences in the location of the EGases at the tissue and cell levels may contribute to the observed variations in their physiological functions. Transgenic *Arabidopsis* overexpressing *PtrCel9A6* produced active proteins with strong hydrolyzing activity toward amorphous cellulose but little or no activity toward crystalline cellulose or other wall polysaccharides. Two other poplar EGases, PopCel1 and PttCel9A/PtrKOR1 (Nakamura and Hayashi, 1993; Master et al., 2004), demonstrate similar substrate specificity for amorphous cellulose which implies the catalytic properties of GH9 enzymes are evolutionarily conserved across the three subfamilies. It is worth noting that all reported enzymatic properties are based on *in vitro* studies using cellulose derivatives and other purified wall polymers. PtrCel9A6 is a glycoprotein and undergoes *N*-glycosylation. However, PtrCel9A6 enzyme activity was not affected by deglycosylation treatment, which suggests the *N*-glycans may not be necessary for its catalytic activity. In plants, *N*-linked glycans usually affect co- and posttranslational folding of the protein as well as directly participate in its active performance (Rayon et al., 1998; Zhao et al., 2013). *N*-glycosylation may be responsible for the correct folding of PtrCel9A6 protein. Once PtrCel9A6 is in its correct folding structure, its activity is not affected by *N*-glycosylation. And this could be the reason why recombinant PtrCel9A6 protein lacked activity in the *E. coli* system.

PtrCel9A6 Is Required in SCW Formation during *Populus* Xylem Differentiation

PtrCel9A6 is mainly expressed in the vascular system of *Populus* as shown by both quantitative RT–PCR and promoter-GUS

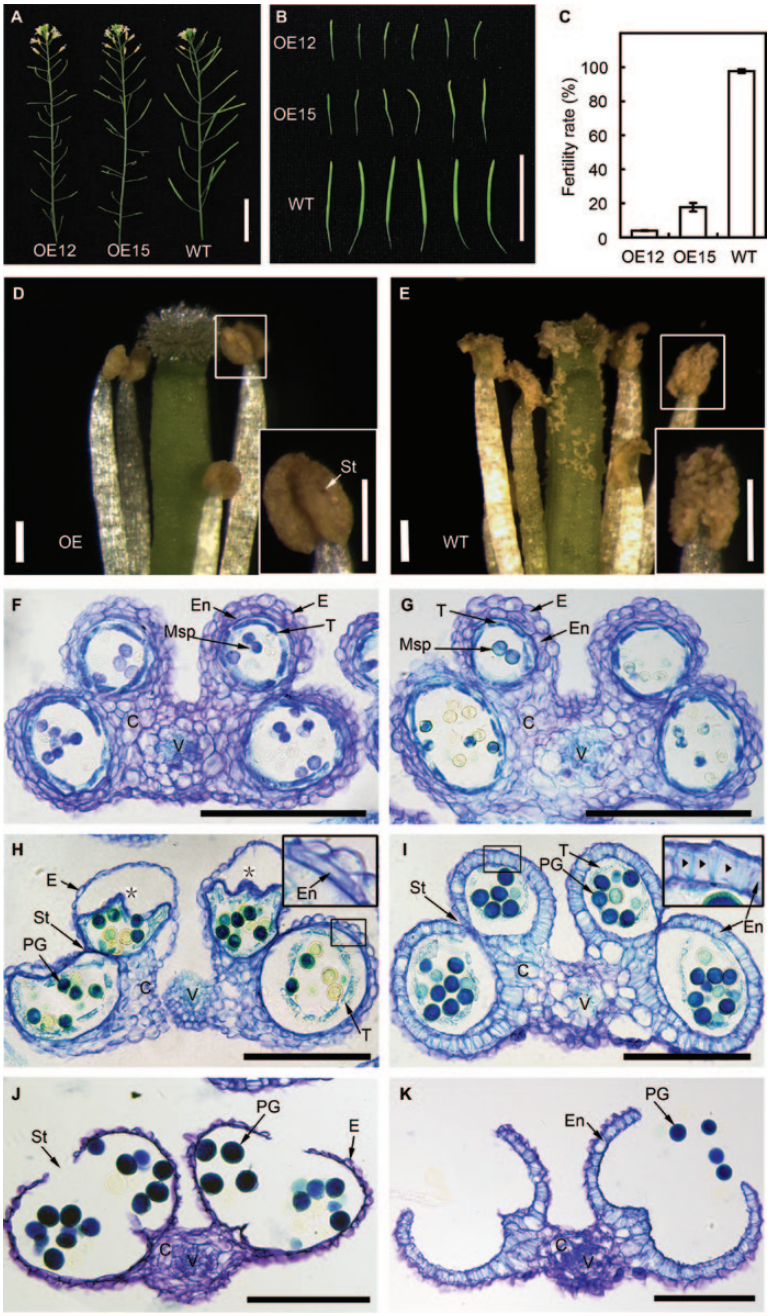

Figure 6. Male Sterility in *PtrCel9A6* Overexpressed *Arabidopsis*.
(A) Shorter and empty siliques in OE compared to wild-type (WT).
(B) Siliques from OE and WT.
(C) Fertility rate in OE and WT plants. The values are means ± SE of 30 plants for each line.
(D) OE plant anthers failed to dehisce and no pollen grains were released.
(E) WT anthers dehisce normally and pollen grains were released. Insets show close-up images of the boxed anthers. Bars = 2 cm in (A, B), 0.2 mm in (D, E).
(F, H, J) Transverse sections of the anther in OE *Arabidopsis* at stages 10, 11, and 13, respectively.
(G, I, K) Anther sections of WT at stages 10, 11, and 13, respectively. At stage 10, no noticeable morphological alterations between OE and WT anthers ((F) versus (G)). (I) Endothecium underwent expansion and quickly deposited cellulose-enriched fibrous bands as well as the tapetum underwent degeneration in WT anther at stage 11. (H) Endothecium in OE anther failed to deposit fibrous bands. Asterisk indicates collapsed endothecium due to failure of thickening. Insets show enlarged images of the boxed endothecium cells. Arrowhead indicates the fibrous bands. (K) Full opening of the stomium to permit pollen release in WT anthers at stage 13. (J) Bilocular anther structure without pollen grain release in OE anthers. E, epidermis; En, endothecium; T, tapetum; Msp, microspores; PG, pollen grains; St, stomium; V, vascular tissue; C, connective. Bars = 100 μm.

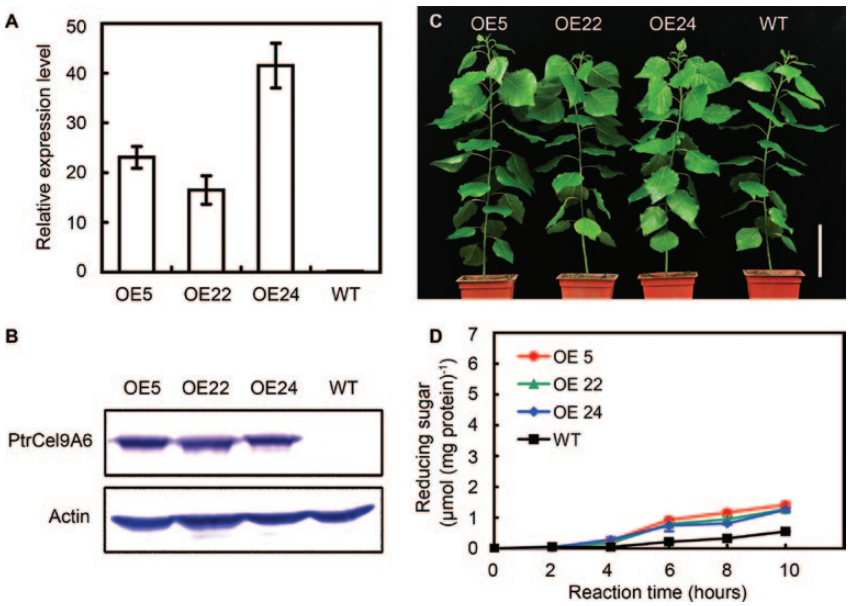

Figure 7. Effect of *PtrCel9A6* Overexpression in *Populus*.
(A) *PtrCel9A6* transcripts were measured by quantitative RT–PCR in *PtrCel9A6*-overexpressed (OE5, OE22, and OE24) and wild-type (WT) *Populus*. The values are means ± SE of three plants of each line.
(B) Western blot detection of PtrCel9A6 proteins in OE and WT leaves. Antibodies against actin as a loading control.
(C) Morphology of OE and WT *Populus* at 8 weeks old. Bar = 10 cm.
(D) Hydrolyzing activity of PtrCel9A6 from transgenic *Populus* and WT. The values are means ± SE of three biological replicates of each line.

staining. In stem, PtrCel9A6 expression was limited to differentiating xylem cells, especially vessel and fiber cells undergoing SCW formation. Significantly thinner SCWs and an irregular xylem phenotype were observed in differentiating poplar xylem when *PtrCel9A6* expression was down-regulated. The transgenic xylem tissue contained significantly less cellulose, a main component of the SCW of wood, compared to the WT.

A number of studies have revealed that KORs, which are γ-subfamily EGases, are essential for cellulose synthesis in plants. KOR has a number of proposed functions including the removal of misaligned glucans, release of CesAs from the growing microfibril, and the unwinding of tension in the helical microfibril (Molhoj et al., 2002; Szyjanowicz et al., 2004; Maloney and Mansfield, 2010). *KOR1* is ubiquitously expressed in *Arabidopsis* (Nicol et al., 1998; Takahashi et al., 2009) and cell wall biosynthesis in *KOR* mutants (*kor*, *acw1*, *rsw2*) is affected throughout the whole plant (Nicol et al., 1998; Lane et al., 2001; Sato et al., 2001). In contrast, *PtrCel9A6* expression is restricted to differentiating xylem tissue, with the highest level being observed in SCW-thickening cells. *PtrCel9A6* down-regulation caused specific SCW biosynthesis defects in the transgenic xylem. Given its specific hydrolysis activity against amorphous cellulose, PtrCel9A6 may function in relation to cellulose synthesis and/or microfibril assembly in the process of xylem cell differentiation. PtrCel9A6 could potentially participate in cellulose synthesis through acting on the cellulose chains undergoing elongation or on the paracrystalline region affecting cellulose microfibril deposition. Recently, a correlation analysis revealed the co-expression of *OsGH9B5* (rice ortholog of *PtrCel9A6*) and *AtGH9B7* (*Arabidopsis* ortholog of *PtrCel9A6*) with *CesA*s in rice and *Arabidopsis*, respectively (Xie et al., 2013). Like KOR, PtrCel9A6 is localized on the plasma membrane, suggesting another possibility that PtrCel9A6 might affect cellulose synthesis through interactions with plasma membrane-localized CesA complexes. Regardless of the mechanism, our results suggest PtrCel9A6 is required for cellulose synthesis in SCW formation during *Populus* xylem differentiation.

Heterologous Expression of *PtrCel9A6* Results in Increased Growth and Male Sterility

Overexpression of PtrCel9A6 in *Arabidopsis* was also found to promote cell expansion and elongation in leaf, root, and vascular tissues. The resulting increase in biomass could result from the involvement of PtrCel9A6 in cell wall loosening which is essential for cell growth. Cellulose–xyloglucan crosslinks are generally believed to be the load-bearing network of the primary cell wall. PtrCel9A6 exhibits substrate specificity for amorphous cellulose and low activity with xyloglucan, suggesting it loosens the cell wall crosslinks through targeting the paracrystalline sites of microfibrils. α-subfamily EGases such as PopCel1 and AtCel1 have been reported to loosen xyloglucans intercalations (Nakamura and Hayashi, 1993; Park et al., 2003; Shani et al., 2004; Hartati et al.,

2008). However, while PopCel1 is localized in the extracellular matrix, PtrCel9A6 is a plasma membrane-bound protein with a catalytic domain that faces the cell wall. Several studies have shown that the cellulose microfibrils in the inner layers undergo extensive reorientation during cell growth, while the reorientation in the outer layers is less pronounced (Carpita and Gibeaut, 1993; McCann and Roberts, 1994; del Campillo, 1999). Overexpression of PtrCel9A6 may result in the modification of the inner layers of the cell wall, resulting in loosened wall structure and enhancement of cell enlargement.

The PtrCel9A6 protein was found to be highly expressed in transgenic poplar trees overexpressing *PtrCel9A6.* However, protein overexpression did not translate to corresponding enzyme activity and no phenotypic alterations were observed in the transgenic trees. The lack of hydrolysis activity could be due to the presence of homologous regulation mechanisms which occurs after protein translation. Evidence from previous studies supports the existence of mechanisms that tightly regulate the homologous activity of EGase genes at different stages of transcription, translation, or post translation (Ohmiya et al., 2003; Park et al., 2003; Shani et al., 2004). For example, heterologous expression of the *Arabidopsis* EGase gene *Cel1* in poplar significantly enhanced the growth of the whole plant, while no phenotypic differences were observed between transgenic and WT plants when it was constitutively overexpressed in *Arabidopsis* (Shani et al., 2004). Our study suggests PtrCel9A6 activity is self-regulated in poplar by posttranslational modification, while the details of the mechanism remain to be further investigated.

Heterologous expression of *PtrCel9A6* in *Arabidopsis* is able to enhance biomass growth and induce male sterility. Overexpression of *PtrCel9A6* in transgenic *Arabidopsis* resulted in a significant, dosage-dependent decrease in fertility rates due to the failure of anthers to open and release pollen. Secondary wall thickening through the deposition of fibrous bands in endothecial cells is required for anther dehiscence, which is driven by the retraction force of the anther wall (Keijzer, 1987; Goldberg et al., 1993). Synthesis of the fibrous bands which consist mainly of cellulose (de Fossard, 1969) occurs during an estimated 42-h period in stage 11 of anther development (Smyth et al., 1990; Sanders et al., 1999). Although little is known about how these fibrous bands are synthesized and deposited in such a short timeframe, one would expect intense cellulose synthesis in the endothecium to occur at this stage which may make it especially sensitive to EGase enzymes. Likely, increased PtrCel9A6 leads to increased EGase activity which interferes with the accumulation of cellulose in the endothecium. Suppression of endothecium thickening prevents the anthers from dehiscing and releasing pollen normally. Though more studies with other plant species are needed, this study demonstrates the potential to use heterologous EGase to engineer plants for biomass enhancement or to develop male-sterility clones in crop breeding.

METHODS

Plant Material

Plant materials in this study (*Populus* and *Arabidopsis*) were grown in a greenhouse or a phytotron with a light and dark cycle of 16 and 8 h at 22°C. *P. trichocarpa* was used for gene cloning and expression analysis. *Populus×euramericana* cv.*'Nanlin895'* was used for genetic transformation according to the protocol used in our lab (Li et al., 2003). *Arabidopsis* (Columbia ecotype) was used for heterologous *PtrCel9A6* gene expression. *Agrobacterium*-mediated transformation of *Arabidopsis* was carried out using a floral dip method (Clough and Bent, 1998).

Analysis of *Populus* GH9 Genes

The *Populus* GH9 family genes from the *Populus* genome database (www.phytozome.net/poplar) were analyzed using the ClustalW method (www.ebi.ac.uk/Tools/msa/clustalw2). The phylogenetic relationship of the PtrGH9 family was analyzed by MEGA version 4 (Tamura et al., 2007) using the neighbor-joining method. Bootstrap values were calculated from 1000 trials. PtrCel9A6 was analyzed for transmembrane domain, signal peptide, and *N*-glycosylation sites using CBS Prediction Servers (www.cbs.dtu.dk/services).

Gene Cloning and Constructs

The full *PtrCel9A6* coding sequence was PCR-amplified and cloned from a cDNA library constructed from *P. trichocarpa* developing xylem tissue. To investigate the genetic function of *PtrCel9A6*, a 248-bp fragment specific to *PtrCel9A6* was constructed to form a hairpin structure under the control of the CaMV 35S promoter, which would function as RNAi suppression in *Populus*. In addition, a full coding region of *PtrCel9A6* cDNA was subcloned into a binary pCambia 2300 vector under the control of an enhanced CaMV 35S promoter. This overexpression construct was introduced into both *Populus* and *Arabidopsis*. Furthermore, a 2.4-kb promoter fragment from the *PtrCel9A6* gene was cloned and fused to a GUS gene for *Populus* transformation. To investigate the subcellular localization of PtrCel9A6, a construct coding for a PtrCel9A6–GFP fusion protein was generated under the control of CaMV 35S promoter, which was then introduced into tobacco leaf through *Agrobacterium*-mediated transformation. The primers used in this study are listed in Supplemental Table 2.

Antibody Production

A variable region encoding a polypeptide from the 316th to 410th amino acid in PtrCel9A6 (indicated in Supplemental Figure 1B) was subcloned into a prokaryotic expression vector pET28b. Expression of the polypeptide and its purification were carried out via a previously established protocol (Song et al., 2010). The recombinant peptide was used as antigens to raise polyclonal antibodies in rabbits. Crude antisera were purified using protein-A Sepharose Cl-4B column and then

used in the study. Anti-Actin monoclonal antibodies were purchased from Abmart (www.ab-mart.com).

Quantitative PT–PCR Analysis

Total RNA was isolated from various tissues using Trizol reagent (Invitrogen, zh.invitrogen.com). Treated with DNase I, the total RNA was used for first-strand cDNA synthesis and then for quantitative RT–PCR analysis of the transcript levels. Quantitative RT–PCR was performed using SYBR Green Master Mix (TOYOBO, www.toyobo-global.com) and an iQ5 Real-Time PCR Detection System (Bio-Rad, www.bio-rad.com). *PtrCel9A6* expression level in each sample was normalized using Actin2 as an internal control.

Western Blot, Microsomal Fraction Preparation, and *N*-Glycosylation Analysis

For Western blot, young leaves of the transgenic plants (*PtrCel9A6*-overexpressed *Populus* and *Arabidopsis*) were ground to fine powder in liquid nitrogen and then dissolved in an equal volume of 2× loading buffer (0.1 M Tris–HCl (pH 6.8), 4% SDS, 0.2% Bromophenol Blue, 20% glycerol). According to methods detailed in our previous study (Song et al., 2010), proteins were immunoblot analyzed using anti-PtrCel9A6 (1:500 dilution) and anti-Actin (1:1000 dilution) antibodies as probes. The microsomal fraction was prepared from *Arabidopsis* leaves overexpressing PtrCel9A6, according to the established protocol (Song et al., 2011). The microsomal fraction was treated with ice-cold 100 mM sodium carbonate (pH 11.5) for 30 min to remove the enclosed proteins and peripheral membrane proteins (Fujiki et al., 1982). Then the suspension was centrifuged at 4°C for 30 min at 200 000 *g* and the pellet was gently rinsed twice with ice-cold distilled water. The proteins were blotted and analyzed.

For the PtrCel9A6 *N*-glycosylation analysis, extracted proteins from transgenic *Arabidopsis* leaves were treated with PNGase F (New England Biolabs, www.neb.com) according to the manufacturer's instructions. Proteins were first incubated with glycoprotein denaturing buffer (0.5% SDS and 40 mM DTT) at 100°C for 10 min. After addition of the G7 reaction buffer (50 mM sodium phosphate, pH 7.5), NP-40 and PNGase F, reaction mix was incubated at 37°C for 2 h. After treatment, the proteins were blotted and analyzed.

Microscopic Analysis

Arabidopsis flowers at different developmental stages were collected and fixed in FAA overnight, dehydrated in graded ethanol series, and embedded into paraffin. Samples were sectioned at 10-μm thickness using a Leica RM2235 rotary microtome (Leica, www.leica-microsystems.com). The sections were stained with toluidine blue and examined under a bright-field microscope (OLYMPUS BX51, www.olympus-global.com). *Populus* and *Arabidopsis* stems were free-hand cross-sectioned, stained with 0.5% phloroglucinol (w/v) in 12% HCl for 3 min, and immediately observed under a bright-field microscope. To observe cell wall structure, *Populus* stems (the 12th internode) were cut into 1-mm lengths for ultrathin sectioning and observed under a transmission electron microscope according to a described protocol (Song et al., 2010). For scanning electron microscopy, *Arabidopsis* leaves were fixed in FAA overnight, dehydrated in graded ethanol series. After critical point drying, mounting, and gold coating, samples were observed under a scanning electron microscope (JEOL JSM-5610LV, www.jeol.com).

GUS Staining and Analysis

PtrCel9A6pro:GUS transgenic *Populus* was examined for GUS activity. Young leaf, root, and stem sections (0.5 cm in length) were incubated in 90% acetone (v/v) for 10 min followed by two rinses with distilled water, and then stained with GUS staining solution (100 mM sodium phosphate (pH 7.0), 10 mm EDTA, 0.5 mm ferricyanide, 0.5 mm ferrocyanide, 0.1% Triton X-100, 20% methanol, and 2 mm X-Gluc) at 37°C. After the GUS signal was developed and the samples were cleared in 70% ethanol, the GUS staining was photographed.

Cellulose Content Analysis and Fiber Length Measurement

The holocellulose and α-cellulose content in the wood of 1-year-old transgenic *Populus* was determined according to the method established in our lab (Hou and Li, 2011). Fiber cell length in transgenic *Arabidopsis* was measured according to published methods (Zawaski et al., 2012) with slight modifications. Briefly, stem segments were treated with equal volumes of glacial acetic acid and 30% (v/v) hydrogen peroxide at 80°C for 6 h with vigorous shaking to separate cells. The resulting pulp was washed three times with distilled water and stained with Safranin O. Fiber cells were mounted on slides and examined under a light microscope (OLYMPUS, BX51, www.olympus-global.com). Fiber length was measured using Image J software.

Enzymatic Activity Assay

Sample was ground in liquid nitrogen to a fine power and homogenized at 4°C in two-fold volume of extraction buffer containing 20 mM sodium phosphate buffer (pH 6.2), 0.5 mM NaCl, and 3 mM phenylmethanesulfonyl fluoride (PMSF). The homogenate was centrifuged at 12 000 *g* for 15 min at 4°C. The supernatant was precipitated in a three-fold volume of ice-cold acetone at –20°C for 1 h, followed by centrifugation. The protein pellet was re-dissolved in the extraction buffer not containing NaCl. The protein preparation was further purified and concentrated through a 30 000-Mr cut-off filter. The protein concentration was measured by BCA Reagent (Tiangen Biotech, www.tiangen.com) using bovine serum albumin (BSA) as a standard. PtrCel9A6 enzymatic activity was assayed using the Dinitrosalicylic Acid (DNS) method (Miller, 1959). In brief, the reaction was initiated with 0.1 mg (1 mg ml^{-1}) enzyme and 0.9 ml 1% (w/v) carboxymethyl cellulose (CMC, medium viscosity, Sigma-Aldrich, www.sigmaaldrich.com) in 20 mM sodium

phosphate buffer (pH 6.2) at 35°C. After reaction, equal volume of DNS reagent was added to the reaction mix and then boiled for 5 min. Absorbance at 540 nm was measured to calculate the reducing sugar produced from enzyme activity using glucose as a reference.

A number of cellulose derivatives and other polysaccharides were used as substrates to examine PtrCel9A6 activity. CMC, Avicel PH101, and xylan from birchwood were purchased from Sigma-Aldrich (www.sigmaaldrich.com). Xyloglucan from tamarind and konjac glucomannan were purchased from megazyme (www.megazyme.com). Phosphoric acid swollen cellulose (PASC) was prepared from Avicel PH101 using 85% (w/v) orthophosphoric acid (Master et al., 2004). All substrates were prepared in 1% (w/v) solutions in 20 mM sodium phosphate buffer (pH 6.2). Enzymatic activity with various substrates was determined at 35°C for 6 h.

SUPPLEMENTARY DATA

Supplementary Data are available at *Molecular Plant Online.*

FUNDING

This work was supported by the National Key Basic Research Program of China (2012CB114502), the National Natural Science Foundation of China (31130012), and Shanghai Science and Technology Commission (11XD1405900) to L.L.

ACKNOWLEDGMENTS

We thank Mr. Xiaoyan Gao for assistance with transmission electron microscopy, Ms. Jiqin Li for scanning electron microscopy, and Mr. Xiaoshu Gao for confocal laser scanning microscopy. No conflict of interest declared.

REFERENCES

Brummell, D.A., and Harpster, M.H. (2001). Cell wall metabolism in fruit softening and quality and its manipulation in transgenic plants. Plant Mol. Biol. **47**, 311–340.

Brummell, D.A., Bird, C.R., Schuch, W., and Bennett, A.B. (1997a). An endo-1,4-beta-glucanase expressed at high levels in rapidly expanding tissues. Plant Mol. Biol. **33**, 87–95.

Brummell, D.A., Catala, C., Lashbrook, C.C., and Bennett, A.B. (1997b). A membrane-anchored E-type endo-1,4-beta-glucanase is localized on Golgi and plasma membranes of higher plants. Proc. Natl Acad. Sci. U S A. **94**, 4794–4799.

Brummell, D.A., Hall, B.D., and Bennett, A.B. (1999). Antisense suppression of tomato endo-1,4-beta-glucanase Cel2 mRNA accumulation increases the force required to break fruit abscission zones but does not affect fruit softening. Plant Mol. Biol. **40**, 615–622.

Carpita, N.C., and Gibeaut, D.M. (1993). Structural models of primary cell walls in flowering plants: consistency of molecular structure with the physical properties of the walls during growth. Plant J. **3**, 1–30.

Clough, S.J., and Bent, A.F. (1998). Floral dip: a simplified method for Agrobacterium-mediated transformation of *Arabidopsis thaliana*. Plant J. **16**, 735–743.

Cosgrove, D.J. (2005). Growth of the plant cell wall. Nat. Rev. Mol. Cell Biol. **6**, 850–861.

de Fossard, R.A. (1969). Development and histochemistry of the endothecium in the anthers of *in vitro* grown *Chenopodium rubrum* L. Bot. Gaz. **130**, 10–22.

del Campillo, E. (1999). Multiple endo-1,4-beta-D-glucanase (cellulase) genes in *Arabidopsis*. Curr. Top. Dev. Biol. **46**, 39–61.

Fujiki, Y., Hubbard, A.L., Fowler, S., and Lazarow, P.B. (1982). Isolation of intracellular membranes by means of sodium carbonate treatment: application to endoplasmic reticulum. J. Cell Biol. **93**, 97–102.

Goldberg, R.B., Beals, T.P., and Sanders, P.M. (1993). Anther development: basic principles and practical applications. Plant Cell. **5**, 1217–1229.

Hartati, S., Sudarmonowati, E., Park, Y.W., Kaku, T., Kaida, R., Baba, K., and Hayashi, T. (2008). Overexpression of poplar cellulase accelerates growth and disturbs the closing movements of leaves in sengon. Plant Physiol. **147**, 552–561.

Henrissat, B. (1991). A classification of glycosyl hydrolases based on amino acid sequence similarities. Biochem J. **280** (Pt 2**),** 309–316.

Horton, R.F., and **Osborne, D.J.** (1967). Senescence abscission and cellulase activity in *Phaseolus vulgaris*. Nature. **214**, 1086–1088.

Hou, S., and Li, L. (2011). Rapid characterization of woody biomass digestibility and chemical composition using near-infrared spectroscopy. J. Integr. Plant Biol. **53**, 166–175.

Keijzer, C.J. (1987). The processes of anther dehiscence and pollen dispersal. New Phytol. **105**, 487–498.

Lane, D.R., Wiedemeier, A., Peng, L., Hofte, H., Vernhettes, S., Desprez, T., Hocart, C.H., Birch, R.J., Baskin, T.I., Burn, J.E., et al. (2001). Temperature-sensitive alleles of RSW2 link the KORRIGAN endo-1,4-beta-glucanase to cellulose synthesis and cytokinesis in *Arabidopsis*. Plant Physiol. **126**, 278–288.

Lashbrook, C.C., Giovannoni, J.J., Hall, B.D., Fischer, R.L., and Bennett, A.B. (1998). Transgenic analysis of tomato endo-beta-1,4-glucanase gene function: role of cel1 in floral abscission. Plant J. **13**, 303–310.

Lashbrook, C.C., Gonzalez-Bosch, C., and Bennett, A.B. (1994). Two divergent endo-beta-1,4-glucanase genes exhibit overlapping expression in ripening fruit and abscising flowers. Plant Cell. **6**, 1485–1493.

Levy, I., Shani, Z., and Shoseyov, O. (2002). Modification of polysaccharides and plant cell wall by endo-1,4-beta-glucanase and cellulose-binding domains. Biomol. Eng. **19**, 17–30.

Li, L., Zhou, Y., Cheng, X., Sun, J., Marita, J.M., Ralph, J., and Chiang, V.L. (2003). Combinatorial modification of multiple lignin traits in trees through multigene cotransformation. Proc. Natl Acad. Sci. U S A. **100**, 4939–4944.

Libertini, E., Li, Y., and McQueen-Mason, S.J. (2004). Phylogenetic analysis of the plant endo-beta-1,4-glucanase gene family. J. Mol. Evol. **58**, 506–515.

Maclachlan, G., and Brady, C. (1994). Endo-1,4-beta-glucanase, xyloglucanase, and xyloglucan endo-transglycosylase activities

versus potential substrates in ripening tomatoes. Plant Physiol. **105**, 965–974.

Maloney, V.J., and Mansfield, S.D. (2010). Characterization and varied expression of a membrane-bound endo-beta-1,4-glucanase in hybrid poplar. Plant Biotechnol. J. **8**, 294–307.

Maloney, V.J., Samuels, A.L., and Mansfield, S.D. (2012). The endo-1,4-beta-glucanase Korrigan exhibits functional conservation between gymnosperms and angiosperms and is required for proper cell wall formation in gymnosperms. New Phytol. **193**, 1076–1087.

Master, E.R., Rudsander, U.J., Zhou, W., Henriksson, H., Divne, C., Denman, S., Wilson, D.B., and Teeri, T.T. (2004). Recombinant expression and enzymatic characterization of PttCel9A, a KOR homologue from *Populus tremula*×tremuloides. Biochemistry. **43**, 10080–10089.

McCann, M.C., and Roberts, K. (1994). Changes in cell-wall architecture during cell elongation. J. Exp. Bot. **45**, 1683–1691.

Miller, G.L. (1959). Use of dinitrosalicylic acid reagent for determination of reducing sugar. Anal. Chem. **31**, 426–428.

Molhoj, M., Pagant, S., and Hofte, H. (2002). Towards understanding the role of membrane-bound endo-beta-1,4-glucanases in cellulose biosynthesis. Plant Cell Physiol. **43**, 1399–1406.

Molhoj, M., Ulvskov, P., and Dal Degan, F. (2001). Characterization of a functional soluble form of a *Brassica napus* membrane-anchored endo-1,4-beta-glucanase heterologously expressed in *Pichia pastoris*. Plant Physiol. **127**, 674–684.

Nakamura, S., and Hayashi, T. (1993). Purification and properties of an extracellular endo-1,4-beta-glucanase from suspension-cultured poplar cells. Plant Cell Physiol. **34**, 1009–1013.

Nakamura, S., Mori, H., Sakai, F., and Hayashi, T. (1995). Cloning and sequencing of a cDNA for poplar endo-1,4-beta-glucanase. Plant Cell Physiol. **36**, 1229–1235.

Nicol, F., His, I., Jauneau, A., Vernhettes, S., Canut, H., and Hofte, H. (1998). A plasma membrane-bound putative endo-1,4-beta-D-glucanase is required for normal wall assembly and cell elongation in *Arabidopsis*. EMBO J. **17**, 5563–5576.

Odonoghue, E.M., and Huber, D.J. (1992). Modification of matrix polysaccharides during avocado (persea-americana) fruit ripening: an assessment of the role of Cx-cellulase. Physiol. Plantarum. **86**, 33–42.

Odonoghue, E.M., Huber, D.J., Timpa, J.D., Erdos, G.W., and Brecht, J.K. (1994). Influence of avocado (persea-americana) Cx-cellulase on the structural features of avocado cellulose. Planta. **194**, 573–584.

Ohmiya, Y., Nakai, T., Park, Y.W., Aoyama, T., Oka, A., Sakai, F., and Hayashi, T. (2003). The role of PopCel1 and PopCel2 in poplar leaf growth and cellulose biosynthesis. Plant J. **33**, 1087–1097.

Ohmiya, Y., Samejima, M., Shiroishi, M., Amano, Y., Kanda, T., Sakai, F., and Hayashi, T. (2000). Evidence that endo-1,4-beta-glucanases act on cellulose in suspension-cultured poplar cells. Plant J. **24**, 147–158.

Park, Y.W., Tominaga, R., Sugiyama, J., Furuta, Y., Tanimoto, E., Samejima, M., Sakai, F., and Hayashi, T. (2003). Enhancement of growth by expression of poplar cellulase in *Arabidopsis thaliana*. Plant J. **33**, 1099–1106.

Pesis, E., Fuchs, Y., and Zauberman, G. (1978). Cellulase activity and fruit softening in avocado. Plant Physiol. **61**, 416–419.

Rayon, C., Lerouge, P., and Faye, L. (1998). The protein N-glycosylation in plants. J. Exp. Bot. **49**, 1463–1472.

Robert, S., Bichet, A., Grandjean, O., Kierzkowski, D., Satiat-Jeunemaitre, B., Pelletier, S., Hauser, M.T., Hofte, H., and Vernhettes, S. (2005). An *Arabidopsis* endo-1,4-beta-D-glucanase involved in cellulose synthesis undergoes regulated intracellular cycling. Plant Cell. **17**, 3378–3389.

Rose, J.K., and Bennett, A.B. (1999). Cooperative disassembly of the cellulose-xyloglucan network of plant cell walls: parallels between cell expansion and fruit ripening. Trends Plant Sci. **4**, 176–183.

Sanders, P.M., Bui, A.Q., Weterings, K., McIntire, K.N., Hsu, Y.C., Lee, P.Y., Truong, M.T., Beals, T.P., and Goldberg, R.B. (1999). Anther developmental defects in *Arabidopsis thaliana* male-sterile mutants. Sex. Plant Reprod. **11**, 297–322.

Sato, S., Kato, T., Kakegawa, K., Ishii, T., Liu, Y.G., Awano, T., Takabe, K., Nishiyama, Y., Kuga, S., Nakamura, Y., et al. (2001). Role of the putative membrane-bound endo-1,4-beta-glucanase KORRIGAN in cell elongation and cellulose synthesis in *Arabidopsis thaliana*. Plant Cell Physiol. **42**, 251–263.

Sexton, R., Durbin, M.L., Lewis, L.N., and Thomson, W.W. (1980). Use of cellulase antibodies to study leaf abscission. Nature. **283**, 873–874.

Shani, Z., Dekel, M., Roiz, L., Horowitz, M., Kolosovski, N., Lapidot, S., Alkan, S., Koltai, H., Tsabary, G., Goren, R., et al. (2006). Expression of endo-1,4-beta-glucanase (cel1) in *Arabidopsis thaliana* is associated with plant growth, xylem development and cell wall thickening. Plant Cell Rep. **25**, 1067–1074.

Shani, Z., Dekel, M., Tsabary, G., and Shoseyov, O. (1997). Cloning and characterization of elongation specific endo-1,4-beta-glucanase (cel1) from *Arabidopsis thaliana*. Plant Mol. Biol. **34**, 837–842.

Shani, Z., Dekel, M., Tsabary, G., Goren, R., and Shoseyov, O. (2004). Growth enhancement of transgenic poplar plants by overexpression of *Arabidopsis thaliana* endo-1,4–0-glucanase (cel1). Mol. Breeding. **14**, 321–330.

Smyth, D.R., Bowman, J.L., and Meyerowitz, E.M. (1990). Early flower development in *Arabidopsis*. Plant Cell. **2**, 755–767.

Song, D., Shen, J., and Li, L. (2010). Characterization of cellulose synthase complexes in *Populus xylem* differentiation. New Phytol. **187**, 777–790.

Song, D., Xi, W., Shen, J., Bi, T., and Li, L. (2011). Characterization of the plasma membrane proteins and receptor-like kinases associated with secondary vascular differentiation in poplar. Plant Mol. Biol. **76**, 97–115.

Szyjanowicz, P.M., McKinnon, I., Taylor, N.G., Gardiner, J., Jarvis, M.C., and Turner, S.R. (2004). The irregular xylem 2 mutant is an allele of korrigan that affects the secondary cell wall of *Arabidopsis thaliana*. Plant J. **37**, 730–740.

Takahashi, J., Rudsander, U.J., Hedenstrom, M., Banasiak, A., Harholt, J., Amelot, N., Immerzeel, P., Ryden, P., Endo, S., Ibatullin, F.M. (2009). KORRIGAN1 and its aspen homolog PttCel9A1 decrease cellulose crystallinity in *Arabidopsis* stems. Plant Cell Physiol. **50**, 1099–1115.

Tamura, K., Dudley, J., Nei, M., and Kumar, S. (2007). MEGA4: molecular evolutionary genetics analysis (MEGA) software version 4.0. Mol. Biol. Evol. **24**, 1596–1599.

Tsabary, G., Shani, Z., Roiz, L., Levy, I., Riov, J., and Shoseyov, O. (2003). Abnormal 'wrinkled' cell walls and retarded development of transgenic *Arabidopsis thaliana* plants expressing endo-1,4-beta-glucanase (cell) antisense. Plant Mol. Biol. **51**, 213–224.

Urbanowicz, B.R., Bennett, A.B., Del Campillo, E., Catala, C., Hayashi, T., Henrissat, B., Hofte, H., McQueen-Mason, S.J., Patterson, S.E., Shoseyov, O., et al. (2007). Structural organization and a standardized nomenclature for plant endo-1,4-beta-glucanases (cellulases) of glycosyl hydrolase family 9. Plant Physiol. **144**, 1693–1696.

Xie, G., Yang, B., Xu, Z., Li, F., Guo, K., Zhang, M., Wang, L., Zou, W., Wang, Y., and Peng, L. (2013). Global identification of multiple OsGH9 family members and their involvement in cellulose crystallinity modification in rice. PLoS One. **8**, e50171.

Zawaski, C., Ma, C., Strauss, S.H., French, D., Meilan, R., and Busov, V.B. (2012). PHOTOPERIOD RESPONSE 1 (PHOR1)-like genes regulate shoot/root growth, starch accumulation, and wood formation in *Populus*. J. Exp. Bot. **63**, 5623–5634.

Zhang, J.W., Xu, L., Wu, Y.R., Chen, X.A., Liu, Y., Zhu, S.H., Ding, W.N., Wu, P., and Yi, K.K. (2012). OsGLU3, a putative membrane-bound endo-1,4-beta-glucanase, is required for root cell elongation and division in rice (*Oryza sativa* L.). Mol. Plant. **5**, 176–186.

Zhao, Y., Song, D., Sun, J., and Li, L. (2013). *Populus* endo-beta-mannanase PtrMAN6 plays a role in coordinating cell wall remodeling with suppression of secondary wall thickening through generation of oligosaccharide signals. Plant J. **74**, 473–485.

Zhou, H.L., He, S.J., Cao, Y.R., Chen, T., Du, B.X., Chu, C.C., Zhang, J.S., and Chen, S.Y. (2006). OsGLU1, a putative membrane-bound endo-1,4-beta-D-glucanase from rice, affects plant internode elongation. Plant Mol. Biol. **60**, 137–151.

Zuo, J., Niu, Q.W., Nishizawa, N., Wu, Y., Kost, B., and Chua, N.H. (2000). KORRIGAN, an *Arabidopsis* endo-1,4-beta-glucanase, localizes to the cell plate by polarized targeting and is essential for cytokinesis. Plant Cell. **12**, 1137–1152.

SUMMARY

This study characterizes a new type of endo-1,4-β-glucanase, PtrCel9A6, which is specifically expressed in developing xylem cells in *Populus*. The results demonstrate that PtrCel9A6 is localized on plasma membrane for remodeling the 1,4-β-glucan chains in the wall matrix and is required for cell wall thickening during xylem differentiation.